AE-250
UDC 621.039.515.15:
621.039.562.24

AE-250

The Interaction Between Control Rods as Estimated by Second-Order One-Group Perturbation Theory

R. Persson

AKTIEBOLAGET ATOMENERGI
STOCKHOLM, SWEDEN 1966

THE INTERACTION BETWEEN CONTROL RODS AS ESTIMATED BY SECOND-ORDER ONE-GROUP PERTURBATION THEORY

Rolf Persson

SUMMARY

The interaction effect between control rods is an important problem for the reactivity control of a reactor. The approach of second-order one-group perturbation theory is shown to be attractive due to its simplicity. Formulas are derived for the fully inserted control rods in a bare reactor. For a single rod we introduce a correction parameter b, which with good approximation is proportional to the strength of the absorber. For two and more rods we introduce an interaction function $g(r_{ij})$, which is assumed to depend only on the distance r_{ij} between the rods. The theoretical expressions are correlated with the results of several experiments in R0, ZEBRA and the Ågesta reactor, as well as with more sophisticated calculations. The approximate formulas are found to give quite good agreement with exact values, but in the case of about 8 or more rods higher-order effects are likely to be important.

Printed and distributed in October, 1966.

LIST OF CONTENTS

1. INTRODUCTION

The effectiveness of a control rod varies with its position in the core, and for a rough estimation of the spatial dependence one mostly uses a first-order perturbation formula. It seems possible to extend the range of validity for the perturbation approach appreciably by introducing a second-order correction in a rather simple way. Knowing the effectiveness of one control rod in a specific position of an otherwise unperturbed core we want to predict the effectiveness of the rod in any other position as well as the combined worth of several similar control rods spread out in arbitrary homologous positions. It seems that the trial formula proposed gives results accurate within a few per cent for the two-dimensional problem. Comparisons are made with more sophisticated calculations [1], [2] and also with several experiments [3], [4], [5], [6].

2. THEORY

2.1 General

The radial dependence of the effectiveness of control rods can be calculated by applying one- or two-group diffusion theory to a homogenized core with appropriate boundary conditions at the rods [1], [7]. Sometimes more sophisticated heterogenenous methods are also used [1].

The simplest approach is to use perturbation theory, which is quite accurate when the perturbations are small. However, control rods cannot be regarded as weak absorbers, and the perturbed flux has to be taken into account. In this paper the one-group perturbation theory has been used, and it is found that the perturbed flux can be corrected for by quite a simple formula.

2.2 A single control rod

Let us assume an unreflected core which is divided in two regions, one narrow region with high absorption (control rod), the rest being the unperturbed part. The buckling change caused by the rod can be expressed as

$$B^2 - B_o^2 = (B_1^2 - B_o^2)\, W_1' \qquad (1)$$

where

B^2 = geometric buckling of the whole system in the critical state,
B_o^2 = material buckling of the unperturbed reference part (index o),
B_1^2 = material buckling of the absorbing region (index 1),
$W_1' = \int_1 \phi\phi'\, dV \Big/ \int_{o+1} \phi\,\phi'\, dV$, modified statistical weight, i.e. the perturbed one-group flux is taken into account,
ϕ = unperturbed flux related to B^2,
ϕ' = perturbed one-group flux.

It may be stressed that eq. (1) is exact as long as the one-group theory is valid, even with big perturbations [8], since the perturbed buckling is taken into account in the weight function. This is, of course, not true with the conventional definition of the statistical weight, which uses the square of the unperturbed flux ϕ.

We introduce the following two parameters:

$$\varepsilon = \frac{\int_1 \phi(\phi - \phi')\, dV}{\int_1 \phi^2\, dV} \qquad (2)$$

and

$$\mu = \frac{\int_{o+1} \phi(\phi - \phi')\, dV}{\int_1 \phi(\phi - \phi')\, dV} \qquad (3)$$

Fig. 1a. shows in graphical form the definition of μ and ε.

The weight W_1' can now be written as

$$W_1' = \frac{(1-\varepsilon)\,\phi_1^2\, V_1}{\int_{o+1} \phi^2\, dV - \mu\,\varepsilon\,\phi_1^2\, V_1} \qquad (4)$$

if we put $\int_1 \phi^2\, dV = \phi_1^2\, V_1$.

When the perturbation is weak, i.e. $\varepsilon \to 0$, we get

$$W_1 = \frac{\phi_1^2 V_1}{\int_{o+1} \phi^2 dV} \tag{5}$$

where W_1 is the conventional statistical weight. By combining eqs. (4) and (5) we find that

$$W_1' = W_1 \cdot \frac{1 - \varepsilon}{1 - \mu \varepsilon W_1} \tag{6}$$

The weights W' and W are consequently related to each other in a simple way. Hitherto we have not applied any condition to μ and ε. We are free to choose the scale of ϕ' relative to that of ϕ, though the form of the flux is determined by the boundary conditions. Let the product $\mu\varepsilon$ be independent of the control rod position. This means, however, that we cannot say anything about μ or ε separately and we have consequently $\mu = \mu(\vec{r}_1)$ and $\varepsilon = \varepsilon(\vec{r}_1)$.

In the following we assume that the geometrical form of the core is a circular cylinder and that the control rod is thin and penetrates the whole core axially. The unperturbed flux ϕ can thus be written as

$$\phi(r, z) = A \sin \alpha z \, J_o(\beta r) \tag{7}$$

where $\alpha = \pi/H$ and $\beta = 2.405/R$. The axial dependence of ϕ in W_1 is eliminated by integration along the whole height of the core.

Since the axial buckling α^2 is the same in all regions we may express the buckling differences as differences between radial bucklings, β_i^2.

Eq. (1) can now be put in the form

$$\delta\beta^2(r) = \delta\beta^2(o) \cdot J_o^2(\beta r) \frac{1 + q(r)}{1 + b\,[1 - J_o^2(\beta r)]} \tag{8}$$

where

$$\delta\beta^2(r) = \beta^2 - \beta_o^2 \tag{8a}$$

$$\delta\beta^2(o) = \frac{(\beta_1^2 - \beta_o^2)(1 - \varepsilon(o))\, V_1}{\int J_o^2\, dV - \mu\varepsilon\, V_1} \tag{8b}$$

$$b = \frac{\mu\varepsilon\, V_1}{\int J_o^2\, dV - \mu\varepsilon\, V_1} \tag{8c}$$

$$q(r) = \frac{\varepsilon(o) - \varepsilon(r)}{1 - \varepsilon(o)} \tag{8d}$$

The constant b and the function q(r) vanish when $\varepsilon = o$, and eq. (8) gives in this case the first-order perturbation formula $\delta\beta^2(r) = \delta\beta^2(o) \cdot J_o^2(\beta r)$. If ε were independent of position, we should have $q(r) = o$. This condition is found to be well fulfilled if $r/R \lesssim 0.35$, in which case $q(r) < 0.01\ b$.

Fig. 1b. shows $\delta\beta^2(r)/\delta\beta^2(o)$ according to eq. (3) versus r/R for strong and weak absorbers.

If we use $1 - J_o^2(\beta r)$ as independent variable and put

$$1 - J_o^2(\beta r) = x \tag{9}$$

eq. (8) can be rewritten as

$$\frac{J_o^2(\beta r)}{\delta\beta^2(r)} = \frac{1}{\delta\beta^2(o)} \left[1 + bx\, \frac{1 - \frac{q(x)}{bx}}{1 + q(x)} \right] \tag{10}$$

This equation can be used to evaluate $\delta\beta^2(o)$, b and q(x) from experiments by means of a graphical method. If $J_o^2(\beta r)/\delta\beta^2(r)$ is plotted versus x, we see that $1/\delta\beta^2(o)$ is the intercept. The slope at $x = o$ gives b, and q(x) is determined from the unlinearity. Experiments show that q(x) is approximately equal to bx^4.

By applying the theory of an eccentric control rod [7] the ratio $\delta\beta^2(r)/\delta\beta^2(o)$ has been calculated under various assumptions in ref. [9]. From these results we can evaluate b versus $\delta\beta^2(o)/\beta^2$ (see fig. 6 and 3.2 below). Due to the limited number of spatial points available in ref. [9] it is impossible to find q(r) from these calculations. There are indications that the relation $q(x) = bx^4$ is too simple, though accurate enough for our purposes.

In reference [9] the ratio $\delta\beta^2(r)/\delta\beta^2(o)$ was fitted to the following trial function, which should be valid when r/R is small:

$$\delta\beta^2(r)/\delta\beta^2(o) = [J_o(\beta r)]^{2 + a \cdot \delta\beta^2(o)} \tag{10a}$$

Here a is a constant.

Eq. (10a) is easily transformed to

$$\frac{J_o^2(\beta r)}{\delta\beta^2(r)} \cdot \delta\beta^2(o) = \{1 - [1 - J_o^2(\beta r)]\}^{-\frac{a}{2}\delta\beta^2(o)} \tag{10b}$$

Since r/R is small, eq. (10b) can be well approximated with

$$\frac{J_o^2(\beta r)}{\delta\beta^2(r)} \cdot \delta\beta^2(o) = 1 + \frac{a}{2}\delta\beta^2(o)\,[1 - J_o^2(\beta r)] \tag{10c}$$

Comparing eqs. (10) and (10c) we find that

$$b = \frac{a}{2} \cdot \delta\beta^2(o) \tag{10d}$$

because q(r) can be neglected close to the center.

According to ref. [9] $a \cong 0.60$ when R = 1.15 m, i.e. $\beta^2 = 4.37$ m^{-2}. This means that

$$b \cong 1.31\,\frac{\delta\beta^2(o)}{\beta^2} \tag{10e}$$

i.e. b is approximately proportional to the relative change of the radial buckling.

2.3 Two control rods

With two control rods in the core we have to consider the interaction effect (see fig. 2). The flux at rod No. 1 is depressed a fraction ε_1 by the rod itself. Rod No. 2 will cause an increased depression at position No. 1 by a fraction $\xi_{12}\varepsilon_2$ of the flux $(1 - \varepsilon_1)\phi_1$. The interaction factor ξ_{12} is, of course, dependent on $\vec{r}_1 - \vec{r}_2$. The perturbed flux ϕ_1' is

$$\phi_1' = (1 - \varepsilon_1)(1 - \xi_{12}\,\varepsilon_2)\phi_1 \tag{11}$$

We get a similar result at position No. 2, viz.

$$\phi_2' = (1 - \xi_{21}\,\epsilon_1)(1 - \epsilon_2)\,\phi_2 \tag{12}$$

The results shown in eqs. (11) and (12) are, as we would expect, independent of the order in which the rods are inserted.

The buckling change caused by the two rods is

$$\beta^2 - \beta_o^2 = (\beta_1^2 - \beta_o^2)\,W_1' + (\beta_2^2 - \beta_o^2)\,W_2' \tag{13}$$

By using eqs. (11) and (12) we can write the weights W_1' and W_2' in the form

$$W_1' = \frac{(1 - \epsilon_1)(1 - \xi_{12}\,\epsilon_2)\,\phi_1^2\,V_1}{\int \phi^2\,dV - \int \phi\,(\phi - \phi')\,dV} \tag{14}$$

$$W_2' = \frac{(1 - \xi_{21}\,\epsilon_1)(1 - \epsilon_2)\,\phi_2^2\,V_2}{\int \phi^2\,dV - \int \phi\,(\phi - \phi')\,dV} \tag{15}$$

The problem is now to find adequate expressions of $\int \phi\,(\phi - \phi')\,dV$. We make an assumption equal to that of eq. (3). With the rods inserted in the order 1 and 2 we get

$$\int_{0+1+2} \phi\,(\phi - \phi')\,dV = \mu\,\epsilon_1\,\phi_1^2\,V_1 + \mu\,\epsilon_2(1 - \xi_{21}\,\epsilon_1)\,\phi_2^2\,V_2 \tag{16}$$

When the rods are inserted in the opposite order, we find that

$$\int_{0+2+1} \phi\,(\phi - \phi')\,dV = \mu\,\epsilon_1\,(1 - \xi_{12}\,\epsilon_2)\,\phi_1^2\,V_1 + \mu\,\epsilon_2\,\phi_2^2\,V_2 \tag{17}$$

Eqs. (16) and (17) have to give the same result and we have consequently

$$\mu(r_1)\,\epsilon_1(r_1)\,\xi_{12}\,\epsilon_2(r_2)\,\phi_1^2\,V_1 = \mu(r_2)\,\epsilon_2(r_2)\,\xi_{21}\,\epsilon_1(r_1)\,\phi_2^2\,V_2 \tag{18}$$

Assuming $V_1 = V_2$ and equal control rods, i.e. $\epsilon_i(r_i) = \epsilon(r_i)$, and bearing in mind that $\mu(r_2)\epsilon(r_2) = \mu(r_1)\epsilon(r_1)$ according to earlier assumptions (p. 5), we get

$$\xi_{12} \cdot \epsilon(r_2)\phi_1^2 = \xi_{21} \cdot \epsilon(r_1)\phi_2^2 \tag{19}$$

Eq. (19) can be rewritten as

$$\frac{\phi_i}{\phi_j}\,\xi_{ij} \cdot \epsilon(r_j) = \frac{\phi_j}{\phi_i}\,\xi_{ji} \cdot \epsilon(r_i) \tag{20}$$

Since ϵ is proportional to $b/(1+b)$ according to eq. (8c) we assume the following trial function:

$$\xi_{ij} \cdot \epsilon(r_j) = \frac{b}{1+b} \cdot \frac{J_o(\beta r_j)}{J_o(\beta r_i)} \cdot g(r_{ij}) \tag{21}$$

The interaction function $g(r_{ij})$ is supposed to depend only on the distance between the rods, i.e.

$$r_{ij} = r_{ji} = |\vec{r}_i - \vec{r}_j|$$

Having two equal control rods, we can express the buckling change according to eq. (13) in the form

$$\frac{\beta^2 - \beta_o^2}{\delta\beta^2(o)} = \frac{[\phi_1^2 - \frac{b}{1+b}\,\phi_1\phi_2 g_{12}][1+q_1] + [\phi_2^2 - \frac{b}{1+b}\,\phi_1\phi_2 g_{12}][1+q_2]}{1 + b[1 - \phi_1^2 - \phi_2^2 + \frac{b}{1+b}\,\phi_1\phi_2 g_{12}]} \tag{22}$$

where

$$\phi_i = J_o(\beta r_i) \tag{22a}$$

$$g_{12} = g_{21} = g(r_{12}) \tag{22b}$$

$$q_i \cong b[1 - J_o^2(\beta r_i)]^4 \tag{22c}$$

Eq. (22) may be rewritten as

$$\frac{\beta^2 - \beta_o^2}{\delta\beta^2(o)} = \phi_1^2 \frac{1+q_1}{1+b[1-\phi_1^2]}\{1+P_{21}\} + \phi_2 \frac{1+q_2}{1+b[1-\phi_2^2]}\{1+P_{12}\} \tag{23}$$

where

$$P_{ij} = \frac{b}{1+b} \frac{\phi_i}{\phi_j} \frac{\phi_i \phi_j - g_{ij}}{1 - \frac{b}{1+b} [\phi_i^2 + \phi_j^2 - \frac{b}{1+b} \phi_i \phi_j g_{ij}]} \tag{24}$$

From eq. (24) it follows that

$$P_{ij} \phi_j^2 = P_{ji} \phi_i^2 \tag{25}$$

The definitions of $\delta\beta^2(o)$, $\underline{b}$ and $g(r_{ij})$ are given in eqs. (8b), (8c) and (21), respectively. The values of the two first quantities are determined from experiments with single rods, whereas $g(r_{ij})$ has to be evaluated from measurements with two rods.

From the definition of $\xi_{ij}\, \epsilon(r_j)$ we have, when $r_j = 0$,

$$\xi_{ij}\, \epsilon(o) = \frac{\phi(r_i) - \phi'(r_i)}{\phi(r_i)} \tag{26}$$

where $\phi'(r_i)$ is the perturbed flux at r_i caused by the rod at $r_j = 0$. According to eq. (21) we get, with $r_{ij} = r_i$,

$$g(r_i) = \frac{1+b}{b} [\phi(r_i) - \phi'(r_i)] / \phi(o) \tag{27}$$

The $g(r_{ij})$ function has been calculated from this expression by means of one-group diffusion theory. Fig. 3 illustrates some steps in the calculation of a relationship between ϕ' and ϕ. We find it convenient to introduce the mean perturbed flux ϕ_p and the asymptotic perturbed flux ϕ_{as}. The parameters r_o/R and $\underline{u}$ appearing in fig. 3 are related, respectively, to ϕ_p and ϕ_{as} and are defined in the appendix, where more details are given. The $g(r_{ij})$ function according to eq. (27) is shown in fig. 7 together with experimental points (see further 3.3).

Eq. (23) shows that the coupling effect between the control rods is taken up by the term P_{ij}. The condition for <u>no interaction</u> is consequently

$$P_{ij} = 0 \tag{28}$$

or according to eq. (24)

$$g(r_{ij}) = J_o(\beta r_i)\, J_o(\beta r_j) \tag{29}$$

The following two cases are investigated.

a) The rods are on the same radius, i.e. $r_i = r_j$.
Eq. (29) then gives

$$g(r_{ij}) = J_o^2(\beta r_i) \tag{30}$$

Eq. (30) can be solved graphically by means of fig. 7 and we find that

$$0.32\ R < r_{ij} < R \tag{31}$$

When the rods are placed symmetrically, i.e. $r_{ij} = 2\, r_i$, we have the lower limit or $r_{ij} = 0.32\ R$.

b) One rod is on the central axis and the other in an eccentric position, i.e. $r_i = 0$, $r_j = r_{ij}$.
Eq. (29) gives

$$g(r_{ij}) = J_o(\beta r_{ij}) \tag{32}$$

We get according to fig. 3 and the appendix

$$r_{ij} = 0.36\ R \tag{33}$$

2.4 Several control rods

When there are more than two control rods we get as a further development of eq. (22)

$$\frac{\beta^2 - \beta_o^2}{\delta\beta^2(o)} = \frac{\sum_i \phi_i^2 [1 + q_i] \prod^{j} [1 - \xi_{ij}\, \epsilon(r_j)]}{1 + b\left\{1 - \sum_i \phi_i^2 \prod^{j \le i} [1 - \xi_{ij}\, \epsilon(r_j)]\right\}} \tag{34}$$

where $\xi_{ij}\, \epsilon(r_j) = 0$ if $j = i$, but otherwise according to eq. (21).

All the quantities of the right-hand side are known from the formulas of one and two control rods.

When there are more than two control rods eq. (34) does not satisfy the condition that the resulting buckling change has to be independent of the order in which the rods are inserted owing to the product with $j \leq i$ in the denominator. In the case of many control rods the denominator of eq. (34) becomes very small and consequently quite sensitive to errors in $\xi_{ij}\, \varepsilon(r_j)$. Since the assumptions on which the formula is based are not exact, it seems better to make a series expansion of eq. (34) such that a separate summation in the denominator is avoided. We get the following second-order expansion, which is analogous to eq. (23) and thus correct for the single- and two-rod cases.

$$\frac{\beta^2 - \beta_o^2}{\delta\beta^2(o)} = \sum_i \phi_i^2 \frac{1 + q_i}{1 + b\,[1 - \phi_i^2]} \{1 + \sum_{j \neq i} P_{ji}\} \tag{35}$$

where

$$q_i \cong b\,[1 - \phi_i^2]^4 \tag{36}$$

$$P_{ij} = \frac{b}{1+b} \frac{\phi_i}{\phi_j} \frac{\phi_i \phi_j - g_{ij}}{1 - \frac{b}{1+b}[\phi_i^2 + \phi_j^2 - \frac{b}{1+b} \phi_i \phi_j g_{ij}]} \tag{37}$$

Assuming $b = 0$ we get from eq. (35) the first-order perturbation formula

$$\frac{\beta^2 - \beta_o^2}{\delta\beta^2(o)} = \sum_i \phi_i^2 \tag{38}$$

If we neglect the second summation in eq. (35) the formula implies merely adding of the single-rod values.

In eqs. (34) - (38) we have used ϕ_i as an abbreviation for $J_o(\beta r_i)$.

3. EVALUATION OF PARAMETERS FROM EXPERIMENTS

3.1 Data on control rods and lattices

Most of the control rods mentioned in ref. [3] have been involved in measurements used here in the evaluation of parameters. Data on the control rods are given in table I. A summary of the conditions studied is presented in table II. In the exponential assembly ZEBRA there was no lattice but only D_2O in order to avoid heterogeneous effects. Earlier lattice experiments in ZEBRA [4] were also analysed, but they are not quoted here owing to rather big experimental errors.

When only reactivity values have been available they have been modified in order to be proportional to buckling differences. The following formulas have been applied [3]:

$$\rho = M^2_{eff}\,\Delta\beta^2 - \frac{L^2_{s,eff}\cdot L^2_{eff}}{(M^2_{eff})^2}\cdot (M^2_{eff}\,\Delta\beta^2)^2 \tag{39}$$

where

$$L^2_{s,eff} = \frac{L^2_s}{1 + L^2_s B^2} \tag{39a}$$

$$L^2_{eff} = \frac{L^2}{1 + L^2 B^2} \tag{39b}$$

$$M^2_{eff} = L^2_{s,eff} + L^2_{eff} \tag{39c}$$

The last term of eq. (39) is only important when the reactivity values are large, since the ratio $L^2_{s,eff}\cdot L^2_{eff}\cdot (M^2_{eff})^{-2} \leq 0.25$.

3.2 Parameters evaluated for single control rods

Single-rod parameters, $\delta\beta^2(o)$, $\underline{b}$ and $q(r)$, were evaluated by means of eq. (10) which was modified into the form

$$\beta^2\cdot\frac{J_o^2(\beta r)}{\delta\beta^2(r)} - \frac{\beta^2}{\delta\beta^2(o)} = \frac{\beta^2}{\delta\beta^2(o)}\cdot bx\,\frac{1 - \frac{q(x)}{bx}}{1 + q(x)} \tag{40}$$

where $x = 1 - J_o^2(\beta r)$. The radial buckling β^2 was introduced for normalization purposes.

The buckling values used in the evaluation are given in tables III - VII. Plots of eq. (40) are shown in figs. 4 and 5. The b values evaluated are plotted versus $\delta\beta^2(o)/\beta^2$ in fig. 6, which also includes a theoretical curve according to section 2.2 and reference [9].

The data of table VIII were taken from ref. [1] and are theoretical. The corresponding measured data [3] have too big error limits to be of interest. Since the data derived from reactivity values are only proportional to the buckling differences, the scale of $\delta\beta^2(o)$ is arbitrary and the corresponding b value is therefore not plotted in fig. 6.

The b values obtained from ZEBRA measurements do not agree with the theoretical curve. The discrepancy may at least partly be due to neutron streaming (anisotropy in the diffusion), which is most pronounced in the exponential assembly. The outer part of the Cd-1 rod consists of aluminium, which is quite transparent to neutrons. However, the SS-3 tube is pure stainless steel. It is also plausible, on the other hand, that in a small assembly like ZEBRA the control rods may no longer be regarded as line absorbers.

3.3 Parameters evaluated for two control rods

The function $g(r_{ij})$ is determined from the interaction effect between two control rods. Three such experiments and one theoretical set of data [1] have been used in this evaluation procedure. The buckling data are given in tables III, IV, VII and VIII and the $g(r_{ij})$ values evaluated are plotted versus r_{ij}/R in fig. 7. The theoretical curve $g(r_{ij})$ with $r_i = r_{ij}$ and $r_j = 0$ is also given (see section 2.3 and appendix).

A trial function of the form

$$g(r_{ij}) = c_o - c_1 \cdot \frac{r_{ij}}{R} + c_2 \left(\frac{r_{ij}}{R}\right)^2 \qquad (41)$$

has been fitted to the experimental points in fig. 7 by a least-squares method. The c values are given in the respective tables. Representative mean values are $c_o = 1.70$, $c_1 = 2.65$ and $c_2 = 1.05$. This curve is also drawn in fig. 7.

The experimental points do not coincide with the theoretical curve, which rather seems to correspond to the lower limit of $g(r_{ij})$. Due to the simplifying assumptions made we cannot expect perfect agreement, but the result shown in fig. 7 nevertheless indicates that the approach seems promising. A mean curve according to eq. (41) may work rather well.

4. APPLICATION OF THEORY TO SEVERAL CONTROL RODS

4.1 Control rods in R0

The control rods called Cd-2 are safety rods in the R0 reactor. Up to six of them have been used simultaneously in experiments [3]. Keeping the water at the critical level of the clean core, various combinations of rods were inserted and the reactivity was determined by pulsed neutron source technique. Since the experimental errors were rather big, the theoretical values [1] had to be preferred for a check of the formula proposed.

The reference values are given in table IX together with values obtained by applying eqs. (34) and (35) with the parameters from table VIII. Both equations give acceptable results. In fig. 8 the results of eq. (35) as well as those of the simple eq. (38) are plotted versus the reference values. The interaction terms are obviously far from negligible.

4.2 Control rods in the Ågesta reactor

The reactivity worths of various combinations of control rods (Cd-Ag-In) in the Ågesta reactor have been studied rather extensively by means of the pulsed neutron source technique [6]. The measurements at 215 °C with fully inserted rods and maximum water level were found suitable for checking the validity of eq. (35). The boundary conditions at an Ågesta control rod have been investigated in the pressurized exponential assembly TZ [10].

The ratio $\delta\beta^2(o)/\beta^2$ was found to be 0.424 in TZ, where the extrapolated radius was 86.3 cm. A transformation [3] to the geometry of the Ågesta reactor ($R_{ex} = 212$ cm) gives $\delta\beta^2(o)/\beta^2 = 0.330$ and thus, according to fig. 6, we have $b = 0.51$. Further we obtain $\delta\beta^2(o) =$

$= 0.424\ m^{-2}$ in the Ågesta reactor. By using theoretical values [11] of L_s^2, L^2 and B^2, i.e. 183 cm^2, 232 cm^2 and 2.94 m^{-2} respectively, we are able to calculate reactivities from buckling changes by means of eq. (39).

We obtain for a control rod placed along the central axis

$$\rho(o) = -391 \cdot 0.424 \cdot 10^{-4}[1 + 0.247 \cdot 391 \cdot 0.424 \cdot 10^{-4}] = -0.01665$$

Since the axial statistical weight of the control rods fully inserted was about 0.95, the effective value of $\rho(o)$ is

$$\rho(o)_{eff} = -0.01580$$

The following set of parameters have been used in eq. (35):

$\delta\beta^2(o) = 0.424 \cdot 0.95 = 0.402\ m^{-2}$

$b = 0.50$

$c_o = 1.70$
$c_1 = 2.65$
$c_2 = 1.05$

} These values correspond to the mean curve shown in fig. 7.

The results are collected in table X. In fig. 9 the experimental values as well as the values according to eq. (35) are plotted versus theoretical values [2]. The systematic difference between the experimental values and the calculated ones may be due to an underestimated value of the migration area.

Another set of parameters may give better agreement between calculated values according to eq. (35) and the "exact" values, but the result seems to indicate that eq. (35) may be too approxamate when there are more than 8 or 10 control rods involved.

Anyhow, from fig. 9 we see that eq. (35) gives a more consistent set of points than eq. (38), i.e. the first-order perturbation formula.

5. CONCLUSIONS

From the material reported here one may conclude that the approximate theory condensed in eq. (35) gives excellent agreement with more exact methods as long as the parameters involved are obtained from single- and two-rod experiments with similar rods in a similar geometry.

The experimental results do not confirm the assumption that the single-rod parameter $\underline{b}$ is a unique function of $\delta\beta^2(o)/\beta^2$. However, there may be systematic errors in the exponential experiments due to the small tank, e.g. anisotropic diffusion and violation of the assumption of line absorbers.

The interaction function $g(r_{ij})$ fitted to experimental points is not quite well reproduced by simple diffusion theory applied to a central control rod. The theoretical curve seems to correspond to a lower limit of $g(r_{ij})$. Due to this and to other approximations the validity of eq. (35) may be dubious when there are more than, say, 8 or 10 control rods involved.

6. ACKNOWLEDGEMENTS

The excellent help of Mr. G Näslund, RFN, with the programming work for parameter fitting and tabulation and of Mr. R Lindh, RFN, with modifications is gratefully acknowledged.

REFERENCES

1. SKARDHAMAR T,
Application of heterogeneous and homogeneous methods in the calculation of control rod effects in D_2O latticies. Physics and Material Problems of Reactor Control Rods. Symposium, Vienna 1963. IAEA, Vienna, 1964, p. 45.

2. SKARDHAMAR T,
Private information

3. BJÖRÉUS K, PERSSON R and WIKDAHL C-E,
Measurements of control rod worths in critical and exponential assemblies. Physics and Material Problems of Reactor Control Rods. Symposium, Vienna 1963. IAEA, Vienna, 1964, p. 173.

4. PERSSON R,
Measurements on control rods in an exponential assembly. 1957.
AB Atomenergi, Dep. of Reactor Physics. (AEF-86.)

5. PERSSON R,
Unpublished experiments.

6. BJÖRÉUS K,
Control rod measurements in the Ågesta reactor with the pulsed neutron method. 1965.
AB Atomenergi, Sweden. (Internal Report - RFT-131)

7. GLASSTONE S and EDLUND M C,
The Elements of Nuclear Reactor Theory.
van Nostrand, Inc., Princeton, N.Y. 1952.

8. PERSSON R,
The evaluation of buckling and diffusion coefficients from two-region experiments.
Exponential and Critical Experiments, Symposium, Amsterdam 1963, IAEA, Vienna, 1964. Vol. 3, p. 289.

9. PERSSON R,
Eccentric test regions in substitution measurements. 1961.
AB Atomenergi, Sweden. (Internal Report - RFX-70).

10. PERSSON R, ANDERSSON A J W and WIKDAHL C-E,
To be published.

11. APELQVIST G,
Calculation of B_m^2 $(\beta; T_m)$ in an Ågesta lattice. 1965.
AB Atomenergi, Sweden. (Internal Report - TPM-RFR-511.)
(Memo in Swedish.)

APPENDIX

Calculations on $g(r_{ij})$

The expression for the buckling change by a single control rod, eq. (8), can be put in the following form:

$$\delta\beta^2(r_1) = (\beta_1^2 - \beta_o^2)\, W_1 \frac{1 - \varepsilon(r_1)}{1 - \frac{b}{1+b} J_o^2(\beta r_1)} \tag{A.1}$$

where we have

$$b = \frac{\mu\varepsilon V_1}{\int_{o+1} J_o^2\, dV - \mu\varepsilon V_1} \tag{A.2}$$

When $r_1 = 0$ we get

$$\delta\beta^2(o) = (\beta_1^2 - \beta_o^2)\, W_1 (1+b)[1 - \varepsilon(o)] \tag{A.3}$$

Bearing in mind the definitions of W_1 and W_1' we see that eqs. (A.1) and (A.3) determine a relationship between the perturbed flux ϕ' and the unperturbed flux ϕ.

We may interpret the effect of the absorber as follows. The flux level is first lowered from ϕ to ϕ_p:

$$\phi_p(r) = \phi(r)\left[1 - \frac{b}{1+b} J_o^2(\beta r_1)\right] \tag{A.4}$$

or if $r_1 = 0$

$$\phi_p(r) = \phi(r)/(1+b) \tag{A.5}$$

The flux ϕ_p is related to the perturbed flux ϕ' by the integral

$$\int \phi\,(\phi_p - \phi')\, r\, dr = 0 \tag{A.6}$$

which follows from the definition of W_1' written as

$$W_1' = \frac{\phi_1 \phi_1' V_1}{\int \phi \phi_p\, dV - \int \phi(\phi_p - \phi')\, dV} \tag{A.7}$$

combined with eqs. (A.1) and (A.4).

Further we define an asymptotic flux ϕ_{as} which is proportional to ϕ and ϕ_p but has the same flux gradient as ϕ' at the outer boundary, i.e.

$$\frac{d\phi_{as}}{dr} /_{r=R} = \frac{d\phi'}{dr} /_{r=R} \tag{A.8}$$

A graphical representation for the case $r_1 = 0$ is given in fig. 3.

The amplitude of ϕ_{as} is determined by means of eq. (A.6), which can be rewritten as

$$\int_o^R \phi(\phi_{as} - \phi_p) r \, dr = \int_o^R \phi(\phi_{as} - \phi') r \, dr \tag{A.9}$$

When $r_1 = 0$ we have

$$\phi = J_o(\beta r) \tag{A.10}$$

$$\phi_p = (1 - \frac{b}{1+b}) J_o(\beta r) \tag{A.11}$$

$$\phi_{as} = (1 - u\frac{b}{1+b}) J_o(\beta r) \tag{A.12}$$

The quantity u in eq. (A.12) has to be determined. Using the definitions according to eqs. (A.10), (A.11) and (A.12) we can put eq. (A.9) in the form

$$\frac{b}{1+b}(1-u) \int_o^R J_o^2(\beta r) r \, dr = (1 - u\frac{b}{1+b}) \int_o^R J_o(\beta r) \frac{\phi_{as}(r) - \phi'(r)}{\phi_{as}(o)} r \, dr \tag{A.13}$$

or, after rearrangement,

$$\frac{1}{b(1-u)} = \frac{\int J_o^2(\beta r) r \, dr}{\int J_o(\beta r) f(r) r \, dr} - 1 \tag{A.14}$$

where

$$f(r) = \frac{\phi_{as}(r) - \phi'(r)}{\phi_{as}(o)} \tag{A.15}$$

The function f(r) has been determined by one-group diffusion theory. Using these results and the relation between $\underline{b}$ and $\delta\beta^2(o)/\beta^2$ (see fig. 6) we find that

$$u \approx 0.65 \tag{A.16}$$

The radius r_o where

$$\phi'(r_o) = \phi_p(r_o) \tag{A.17}$$

is now obtained by using eqs. (A.11), (A.12) and (A.16), which give

$$\frac{\phi'(r_o)}{\phi_{as}(r_o)} = \frac{1}{1 + 0.35\ b} \tag{A.18}$$

and

$$\frac{\phi_{as}(r_o) - \phi'(r_o)}{\phi_{as}(o)} = \frac{0.35\ b}{1 + 0.35\ b} \cdot J_o(\beta r_o) \tag{A.19}$$

The solution of eq. (A.19) gives

$$r_o \approx 0.36\ R \tag{A.20}$$

Eqs. (A.16) and (A.20) afford us some help in plotting $g(r_{ij})$. According to the definition

$$\xi_{ij}\, \epsilon(o) = \frac{\phi(r_i) - \phi'(r_i)}{\phi(r_i)} \tag{A.21}$$

we find that

$$\frac{b}{1+b} \cdot g(r_{ij}) = \phi(r_i) - \phi'(r_i) \tag{A.22}$$

where $r_{ij} = r_i$. Eqs. (A.8), (A.12) and (A.16) together with eq. (A.22) show that

$$\lim_{r_{ij} \to R} g(r_{ij}) = 0.65\, J_o(\beta r_{ij}) \qquad (A.23)$$

At $r_{ij} = r_o$ eq. (A.22) combined with eqs. (A.17) and (A.20) gives

$$g(r_o) = J_o(\beta r_o) \qquad (A.24)$$

or

$$g(r_o) = 0.821 \qquad (A.25)$$

Table I. Control rod data

Symbol*	Composition OD cm	ID cm	Material	Remarks
Cd-1	7.5	6.9	Al	
	6.9	6.7	Cd	
	6.5	5.9	Al	
Cd-2	2.8	2.5	S.S.	Length 1.30 m
	2.5	2.0	Cd	
	2.0	1.7	S.S.	
Cd-Ag-In	10.4	10.0	S.S.	5 % Cd, 80 % Ag, 15 % In
	10.0	9.4	Cd-Ag-In alloy	
	9.4	8.8	S.S.	
SS-3	6.0	5.1	S.S.	$\Sigma_a(2200) = 3.40 \pm 0.05$ mm^2/g

* The same symbols as in ref. [3].

Table II. Summary of control rod measurements analysed

Fuel: U 3.05 cm in Al, OD 3.45 cm, ID 3.15 cm

Control rod Symbol	Internal material	No. of rods	Square lattice pitch cm	Facility	Tables and figures where the results of the analysis are given
Cd-1	D_2O	1, 2	(D_2O)	ZEBRA	Table III, figs. 4, 6, 7
SS-3	D_2O	1, 2	(D_2O)	"	" IV, " " " "
Cd-1	air	1	15	R0	" V, " 5, 6
	air	1	17	"	" " " " "
	D_2O	1	17	"	" " " " "
Cd-Ag-In	air	1	15	"	" VI, " " "
	air	1	17	"	" " " " "
SS-3	D_2O	1, 2	17	"	" VII, " " ", 7
Cd-2	D_2O	1, 2	19	"	" VIII, " " "

Table III. Cd-1 in ZEBRA

Only D_2O: R = 52.05 cm

x/y cm	$\delta\beta^2_{exp}$ m^{-2}	$\delta\beta^2_{fitted}$ m^{-2}	Fitted parameters
0/0	11.50 ± 0.05	11.52	
10/10	8.43	8.28	$\delta\beta^2(o) = 11.518 \pm 0.05$
10/10	8.28	8.28	$b = 0.608 \pm 0.03$
10/20	5.23	5.25	
10/30	2.59	2.66	
10/0; 20/0	11.83	11.76	
" 30/0	11.44	11.32	
" -10/0	19.54	20.19	
" -10/20	16.18	16.23	
" -10/-20	16.03	16.23	$c_o = 1.46 \pm 0.06$
" -20/0	18.40	18.26	$c_1 = 1.59 \pm 0.25$
" -20/10	17.62	17.28	$c_2 = 0.05 \pm 0.26$
" -20/-10	17.48	17.28	
" 20/30	11.52	11.57	
" -30/0	14.94	15.02	

Table IV. SS-3 in ZEBRA

Only D_2O; R = 52.05 cm

x/y cm	$\delta\beta^2_{exp}$ m^{-2}	$\delta\beta^2_{fitted}$ m^{-2}	Fitted parameters
0/0	5.07 ± 0.06	5.07	
10/10	3.91	3.90	$\delta\beta^2(o) = 5.072 \pm 0.04$
15/15	2.78	2.80	$b = 0.231 \pm 0.05$
20/25	1.28	1.27	
20/0; 20/15	4.61	4.64	
" -10/0	7.64	7.74	
" -10/25	5.18	5.07	
" -20/-10	5.98	5.93	
" -20/-20	5.06	4.94	$c_o = 1.66 \pm 0.32$
" -30/0	4.36	4.73	$c_1 = 2.41 \pm 0.73$
" -30/-30	3.30	3.31	$c_2 = 0.99 \pm 0.40$
" -39.5/0	3.55	3.56	
30/0; -10/25	3.59	3.54	
35/0; -30/0	2.50	2.50	
" -30/-30	1.26	1.23	
" -35/25	1.17	1.19	

Table V. Cd-1 in R0

Fuel: U 3.05 cm

x/y cm	$\delta\beta^2_{exp}$ m^{-2}	$\delta\beta^2_{fitted}$ m^{-2}	Remarks
0/0	1.347	1.343	Cd-1 (air)
0/15	1.246	1.250	15.0 cm lattice (R = 114.0 cm)
0/30	1.006	1.009	$\delta\beta^2(o) = 1.343 \pm 0.005$
0/45	0.724	0.717	$b = 0.453 \pm 0.025$
0/60	0.450	0.455	
0/0	1.371	1.361	Cd-1 (air)
0/17	1.242	1.244	17.0 cm lattice (R = 115.0 cm)
0/34	0.950	0.957	$\delta\beta^2(o) = 1.361 \pm 0.007$
0/51	0.633	0.628	$b = 0.419 \pm 0.030$
0/68	0.367	0.356	
17/17	1.126	1.139	
34/34	0.685	0.682	
51/51	0.304	0.301	
68/68	0.068	0.062	
0/0	1.419	1.416	Cd-1 (D_2O)
0/17	1.291	1.290	17.0 cm lattice (R = 115.0 cm)
17/17	1.169	1.177	$\delta\beta^2(o) = 1.416 \pm 0.005$
17/34	0.903	0.901	$b = 0.478 \pm 0.024$
34/34	0.697	0.697	
51/51	0.306	0.308	
51/68	0.165	0.159	
68/68	0.078	0.064	

Table VI. Cd-Ag-In (air) in R0

Fuel: U 3.05 cm

x/y cm	$\delta\beta^2_{exp}$ m^{-2}	$\delta\beta^2_{fitted}$ m^{-2}	Remarks
0/0	1.801	1.792	15.0 cm lattice
0/15	1.646	1.655	R = 114 cm
0/30	1.305	1.313	$\delta\beta^2(o) = 1.792 \pm 0.008$
0/45	0.918	0.914	$b = 0.602 \pm 0.033$
0/60	0.585	0.577	
0/0	1.828	1.812	17.0 cm lattice
0/17	1.641	1.634	R = 115.0 cm
0/34	1.201	1.214	$\delta\beta^2(o) = 1.812 \pm 0.013$
0/51	0.790	0.774	$b = 0.660 \pm 0.044$
0/68	0.453	0.441	
17/17	1.440	1.476	
17/34	1.096	1.104	
34/34	0.851	0.843	
34/51	0.571	0.559	
51/51	0.381	0.376	
51/68	0.206	0.199	
68/68	0.095	0.081	

Table VII. SS-3 (D_2O) in R0

Fuel: U 3.05 cm. Lattice: 17.0 cm

x/y cm	$\delta\beta^2_{exp}$ m^{-2}	$\delta\beta^2_{fitted}$ m^{-2}	Fitted parameters
0/0	0.631	0.632	
0/17	0.587	0.585	
17/17	0.541	0.542	$\delta\beta^2 = 0.632 \pm 0.001$
34/34	0.339	0.339	$b = 0.216 \pm 0.010$
51/51	0.150	0.149	
68/68	0.029	0.029	
0/0 ; 0/-17	1.105	1.115	
0/17; 0/-17	1.170	1.161	
0/17; 0/-34	1.094	1.092	
0/34; 0/-34	1.001	0.998	$c_o = 1.68 \pm 0.03$
0/34; 0/-51	0.844	0.844	$c_1 = 2.72 \pm 0.08$
0/51; 0/-51	0.682	0.683	$c_2 = 1.11 \pm 0.05$
0/51; 0/-68	0.527	0.527	
0/68; 0/-68	0.374	0.377	
0/68; 0/-85	0.261	0.260	
0/85; 0/-85	0.151	0.151	

Table VIII. Cd-2 in R0 (R = 115.0 cm)

1 and 2 control rods

$k \cdot \delta\beta^2_{exact}$ corresponds to theoretical reactivity values [1] which have been corrected in order to be proportional to buckling differences

x/y cm	$k \cdot \delta\beta^2_{exact}$	$k \cdot \beta^2_{fitted}$	Evaluated parameters
0/19	1805	1802	
0/-38	1345	1351	
-38/19	1225	1226	$\delta\beta^2(o) = 1983 \pm 8$
-38/-38	920	914	$b = 0.204 \pm 0.016$
0/-57	830	828	
57/-57	300	307	
0/19; 0/-38	3275	3283	
0/19; 0/-57	2770	2765	
-38/19; 38/19	2585	2589	$c_o = 1.66 \pm 0.05$
-38/19; 38/-38	2300	2296	$c_1 = 2.57 \pm 0.15$
0/-38; 38/-38	2130	2123	$c_2 = 1.02 \pm 0.10$
38/19; 38/-38	2110	2119	
-38/19; 57/-57	1595	1596	
38/19; 57/-57	1535	1533	

See further table IX which gives the values with 3, 4 and 6 control rods.

Table IX. Cd-2 in R0 (R = 115.0 cm)

3, 4 and 6 control rods

Values of 1 and 2 control rods are given in table VIII from which the following parameters are taken

$$\delta\beta^2(o) = 1983; \quad b = 0.204$$

$$c_o = 1.66; \quad c_1 = 2.57; \quad c_2 = 1.02$$

$k \cdot \delta\beta^2_{exact}$ corresponds to reactivity values given in ref. [1].
Figures within parenthesis: $100(\delta\beta^2_{fitted} - \delta\beta^2_{exact})/\delta\beta^2_{exact}$

x/y cm	$k \cdot \delta\beta^2_{exact}$	$k \cdot \delta\beta^2_{fitted}$ acc. to eq. (34)	acc. to eq. (35)	acc. to eq. (38)
-38/19; 38/19 38/-38	3670	3652 (-0.5)	3637 (-0.9)	3610 (-1.6)
0/19; 38/19 0/-38	4530	4636 (+2.3)	4530 (0)	4565 (+0.8)
38/19; 0/-38 38/-38	3445	3435 (-0.3)	3442 (-0.1)	3729 (+8.2)
-38/19; 0/19 38/19	4170	4199 (+0.7)	4206 (+0.9)	4446 (+6.6)
-38/-38; 0/-38 38/-38	2940	2928 (-0.4)	2936 (-0.1)	3416 (+16.2)
-38/19; 38/19 -38/-38; 38/-38	4785	4783 (0)	4725 (-1.3)	4605 (-3.8)
0/19; 38/19 0/-38; 38/-38	5390	5384 (-0.1)	5394 (+0.1)	5560 (+3.2)
-38/19; 0/19 38/19; -38/-38 0/-38; 38/-38	8045	8131 (+1.1)	7992 (-0.7)	7862 (-2.3)

Table X. Cd-Ag-In in Ågesta (R = 212 cm)

Number of control rods						ρ(exp.) [6] pcm	ρ(theor.) [2] pcm	ρ(approx.) pcm	
r_1	r_2	r_3	r_4	r_5	Total			b = 0.50	b = 0
	4				4	6535	-	5140	5270
		4			4	6080	-	4670	4300
1	4				5	6870	5880	5390	6900
1		4			5	7375	6620	5920	5920
1			4		5	6210	5460	4660	4360
	4	4			8	10450	9260	8840	9690
			4	4	8	5970	5060	4440	4940
1	4	4			9	10980	9530	8710	11350
	4	4	4		12	15400	14080	11890	12580
		4	4	4	12	13770	11430	9090	9350
	4	4	4	4	16	19100	16770	13850	14870

$r_1 = 0$
$r_2 = 54$ cm
$r_3 = 54\sqrt{2}$ cm
$r_4 = 108$ cm
$r_5 = 54\sqrt{5}$ cm

ρ(approx.) was obtained by means of eqs. (35) and (39)

$\delta\beta^2(o) = 0.402\ m^{-2}$
$c_o = 1.70$
$c_1 = 2.65$
$c_2 = 1.05$

$L_s^2 = 183\ cm^2$
$L^2 = 232\ cm^2$
$B^2 = 2.94\ m^{-2}$
$pcm = 10^{-5}$

LEGEND TO THE FIGURES

Fig. 1. A single control rod. a) Definition of μ and ε. b) Radial dependence of weight function.

Fig. 2. Two control rods. a) Definition of ξ_{ij} ε_j. b) Weight functions of two control rods placed symmetrically. $\delta\beta^2(o)$ refers to the value of a single control rod.

Fig. 3. Definition of fluxes with a control rod at $r = 0$.

Fig. 4. Single-rod measurements in ZEBRA. Graphical representation.

Fig. 5. Single-rod measurements in R0. Graphical representation.

Fig. 6. The single-rod parameter $\underline{b}$ versus the maximum relative change or the radial buckling, $\delta\beta^2(o)/\beta^2$.

Fig. 7. The interaction function $g(r_{ij})$ versus the rod-to-rod spacing, r_{ij}/R.

Fig. 8. Approximate values of buckling versus exact values with various combinations of control rods Cd-2 in R0.

Fig. 9. Control rods in the Ågesta reactor. The reactivity ratios ρ(approx.)/ρ(theor.) and ρ(exp.)/ρ(theor.) vs ρ(theor.).

1a)

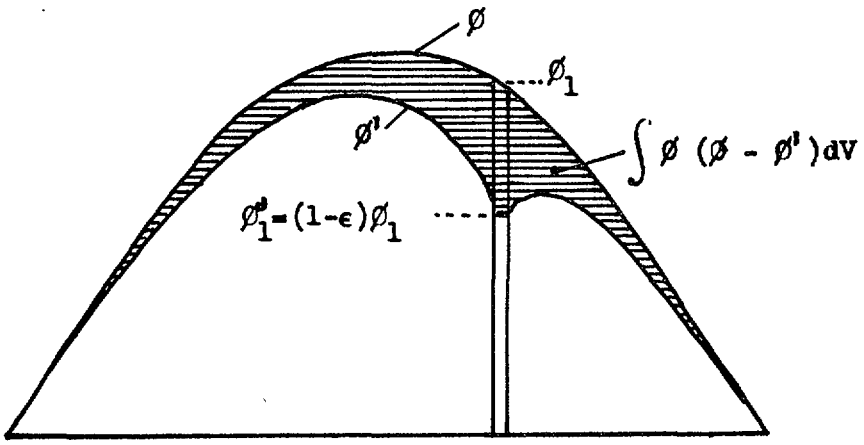

$$\mu = \frac{\int_{o+1} \phi\ (\phi - \phi')dV}{\int_{1} \phi\ (\phi - \phi')dV} = \frac{\int_{o+1} \phi\ (\phi - \phi')dV}{\phi_1\ (\phi_1 - \phi_1')V_1}$$

$$\epsilon = \frac{\phi_1 - \phi_1'}{\phi_1} \quad \text{gives} \quad \mu\epsilon\phi_1^2\, V_1 = \int_{o+1} \phi\ (\phi - \phi')dV$$

1b)

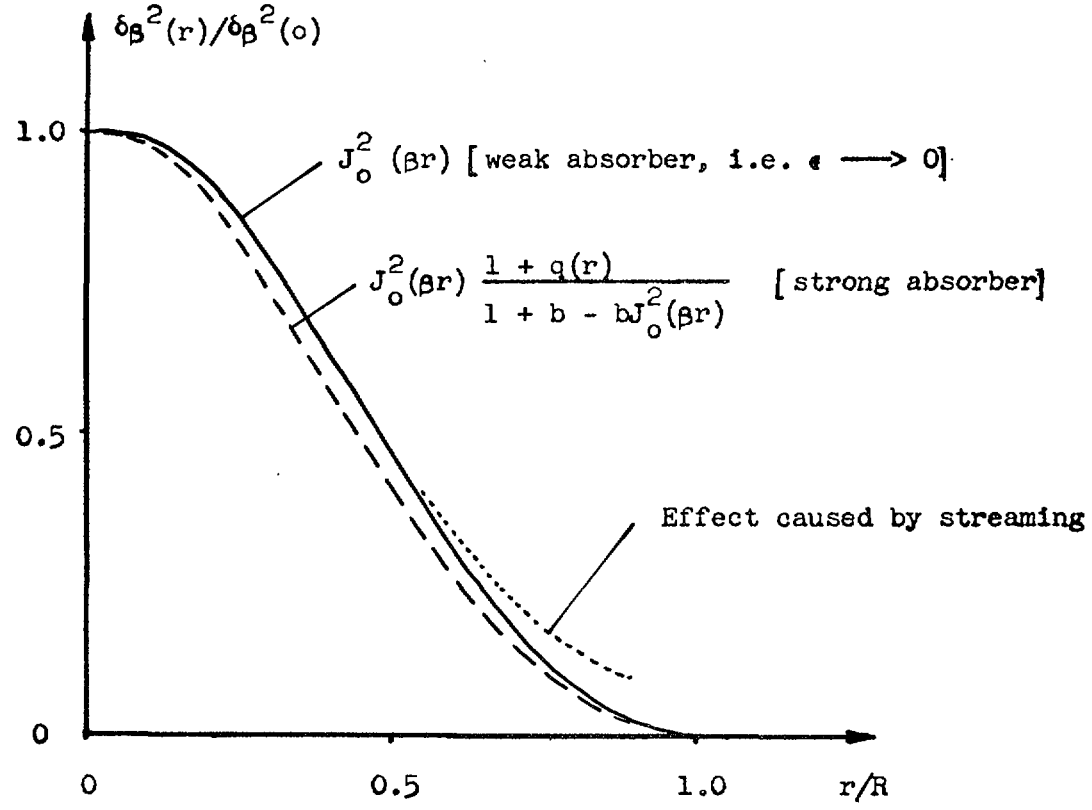

Fig. 1. A single control rod

a) Definition of μ and ϵ

b) Radial dependence of weight function

2a)

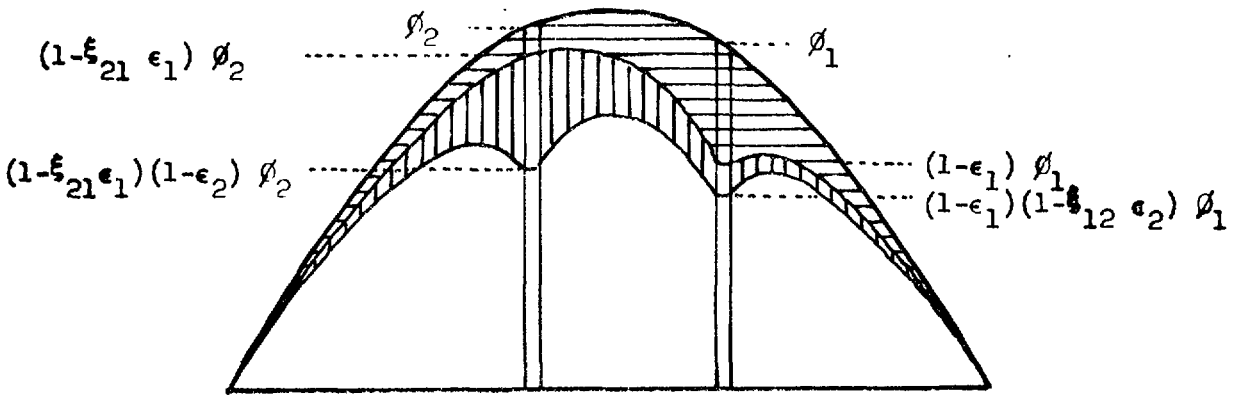

2b)

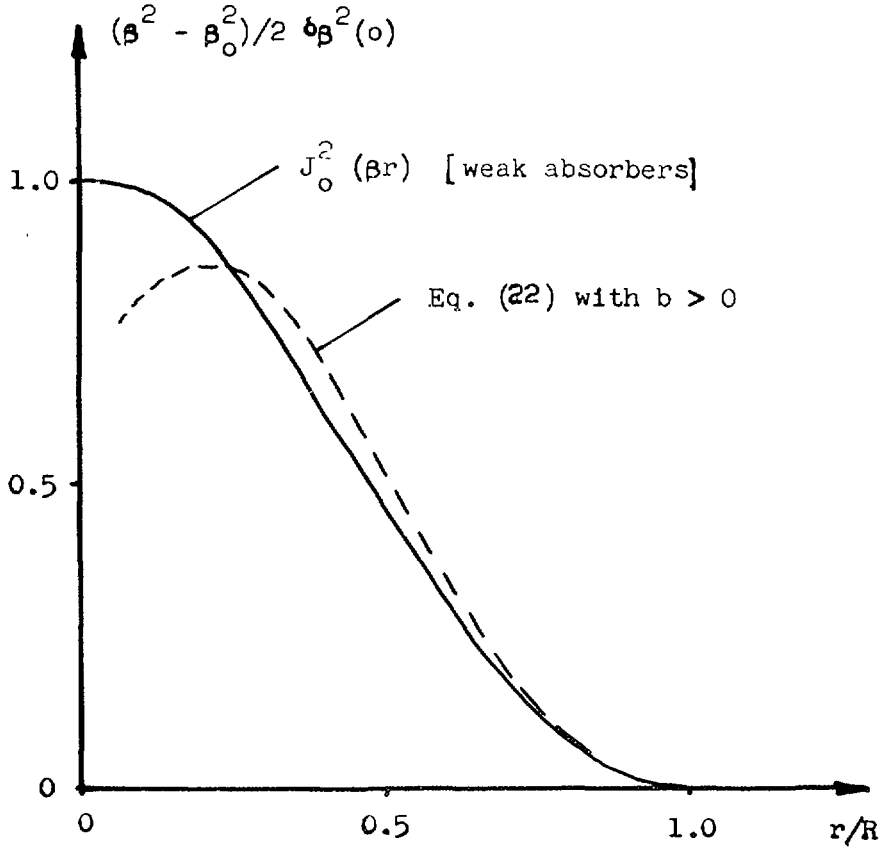

Fig. 2. Two control rods

a) Definition of $\xi_{ij}\ \epsilon_j$

b) Weight functions of two control rods placed symmetrically. $\delta\beta^2(o)$ refers to the value of a single control rod

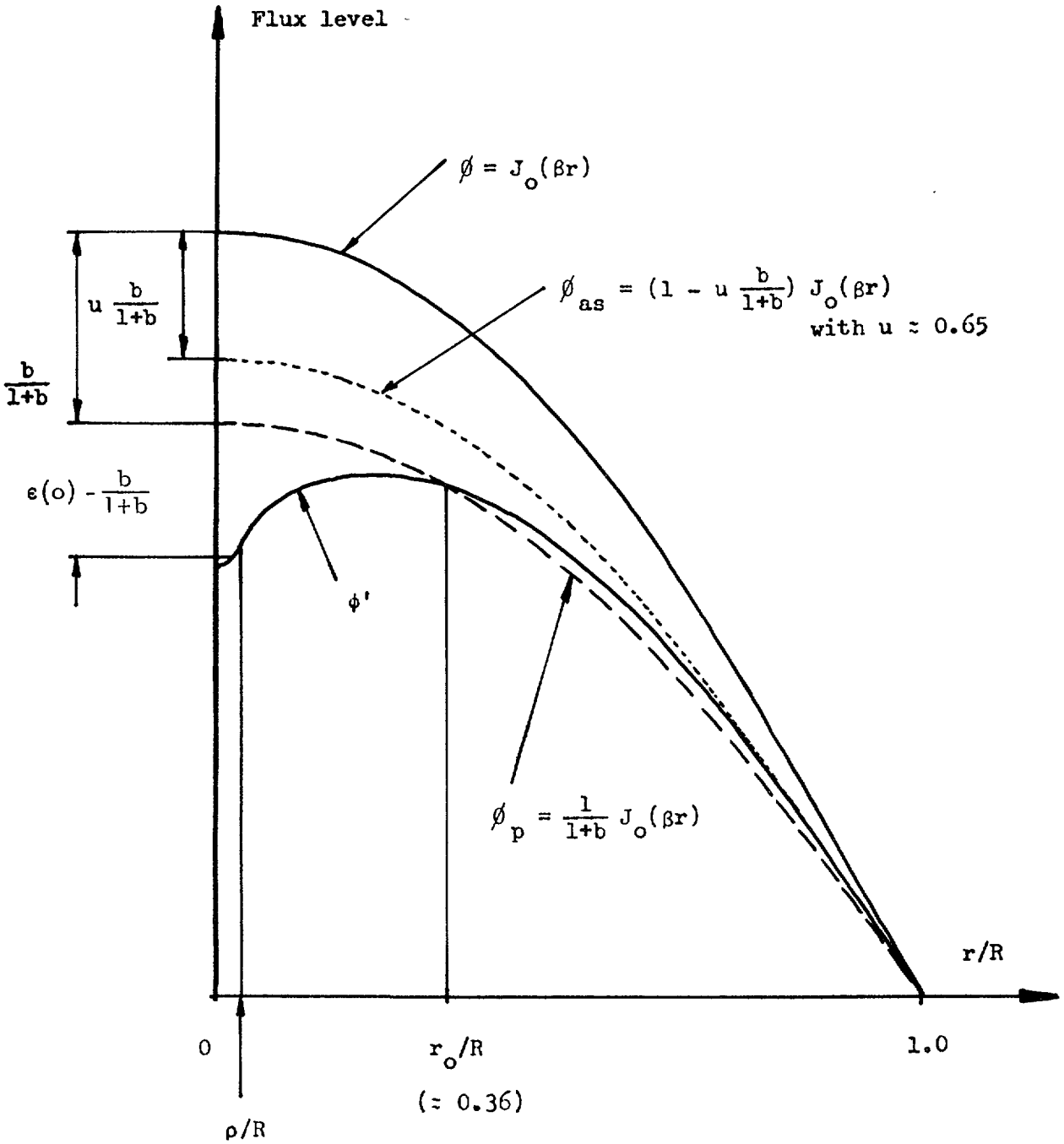

$$\delta\beta^2(o) = (\beta_1^2 - \beta_o^2)\, W_1' \quad \text{where } W_1' = \frac{\phi_1\, \phi_1'\, V_1}{\int_{0+1} \phi\, \phi_p\, dV}$$

$$\left(\frac{d\phi'}{dr}\right)_{r=R} = \left(\frac{d\phi_{as}}{dr}\right)_{r=R}$$

Fig. 3. Definition of fluxes with a control rod at r = 0

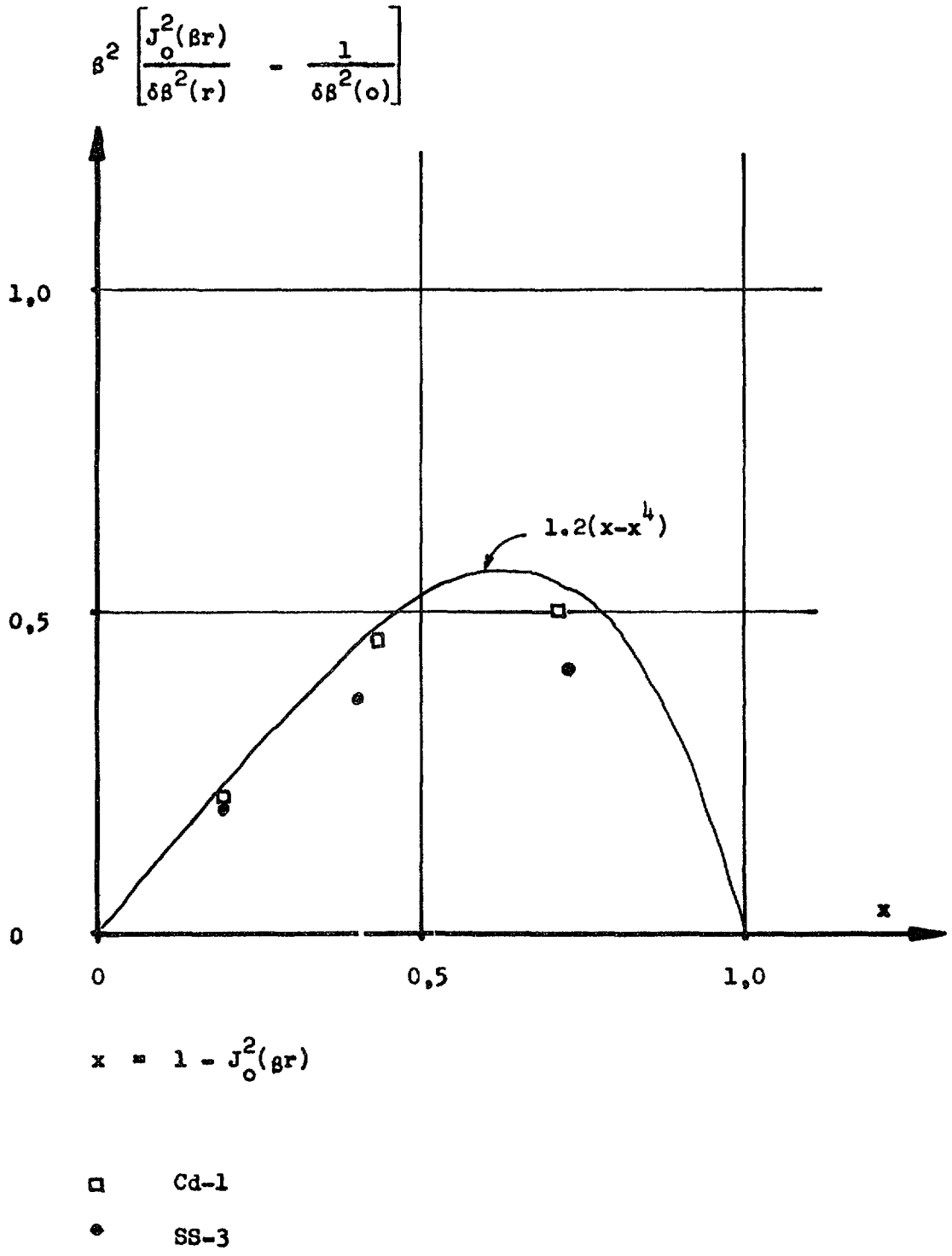

Fig. 4. Single-rod measurements in ZEBRA. Graphical representation

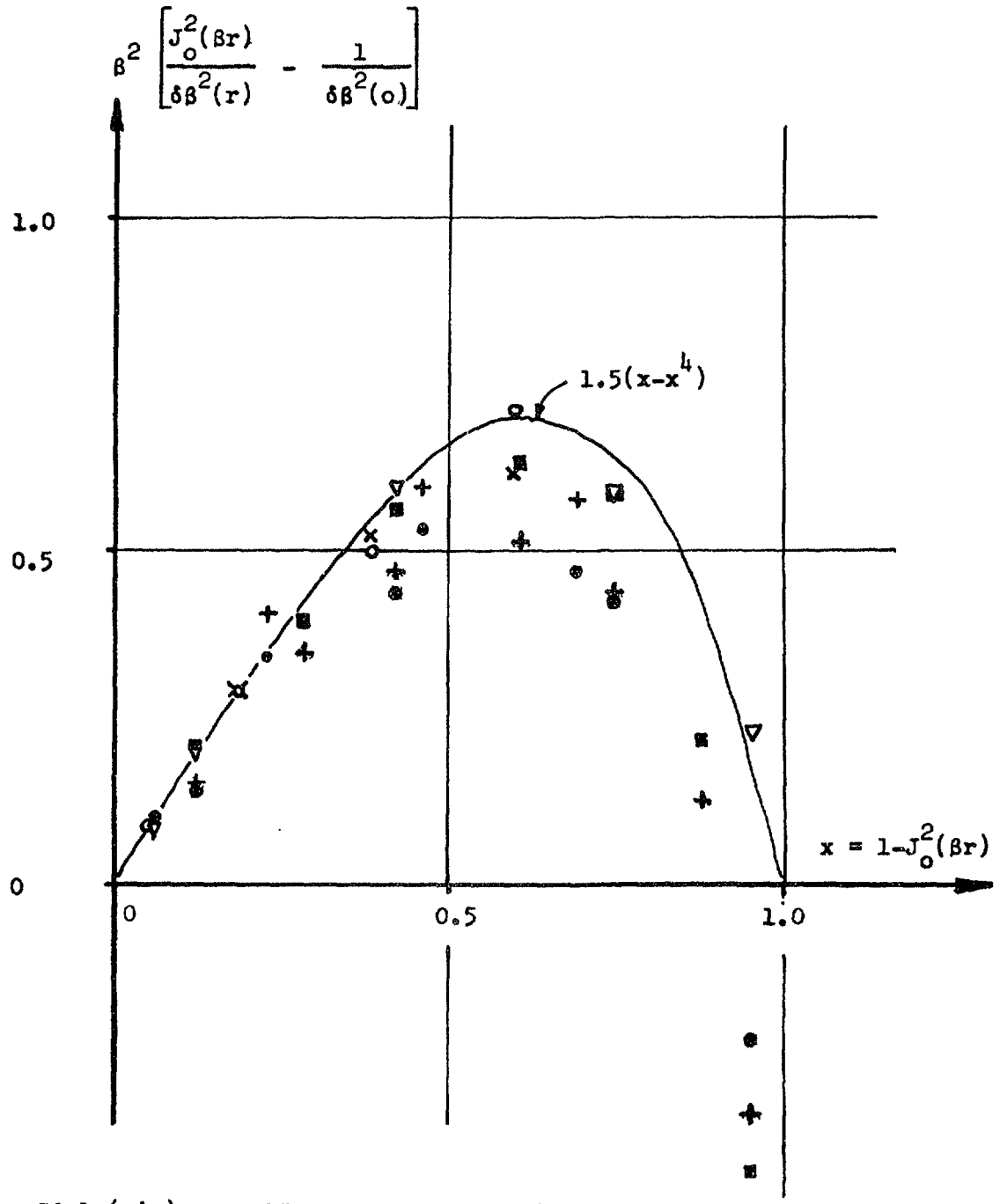

o	Cd-1 (air)	15.0 cm	square	lattice	
x	AgInCd (air)	"	"	"	"
•	Cd-1 (air)	17.0	"	"	"
+	AgInCd (air)	"	"	"	"
■	Cd-1 (D_2O)	"	"	"	"
▽	SS-3 (D_2O)	"	"	"	"

Fig. 5. Single-rod measurements in R0. Graphical representation

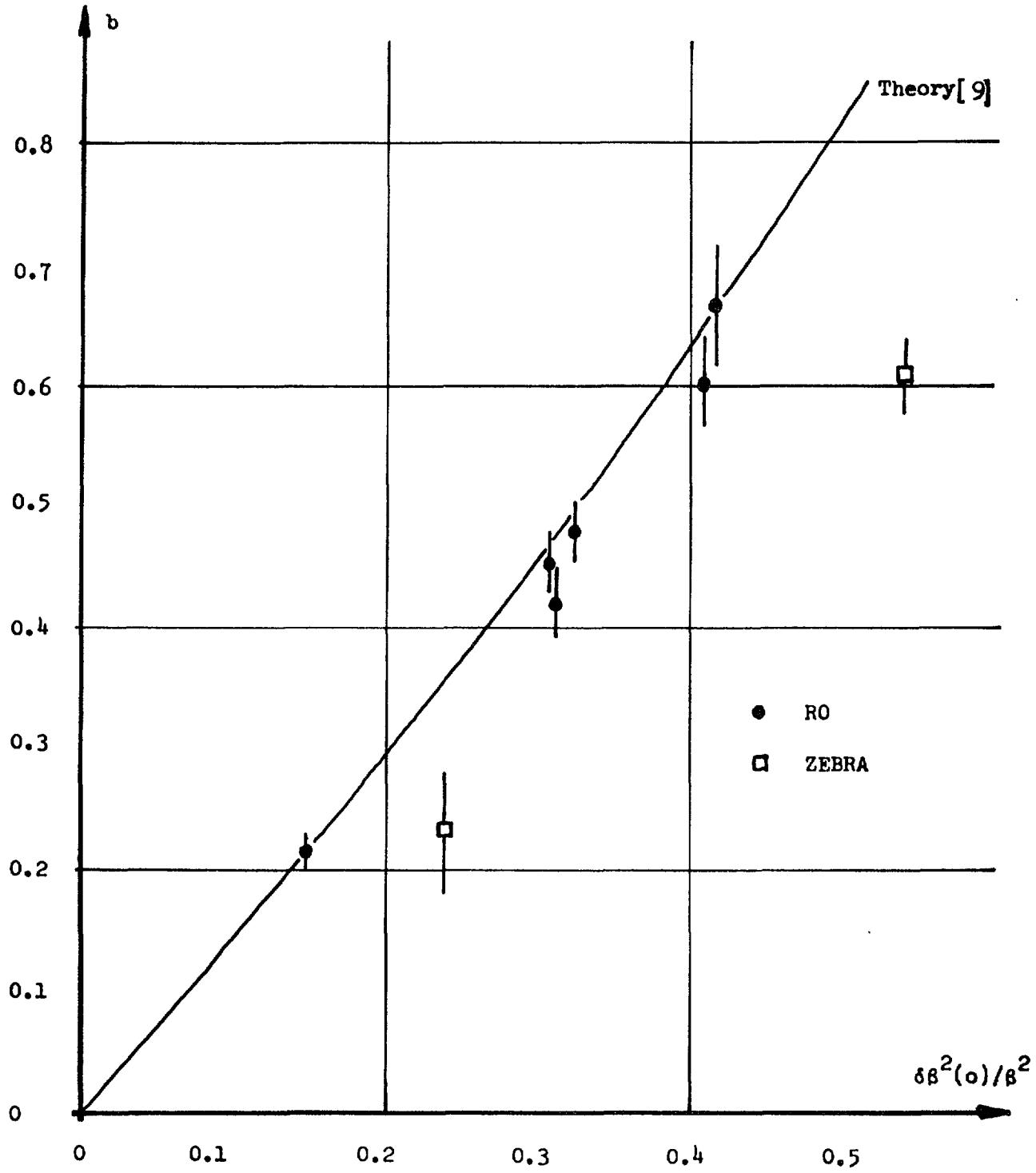

Fig. 6. The single-rod parameter b versus the maximum relative change of the radial buckling, $\delta\beta^2(o)/\beta^2$

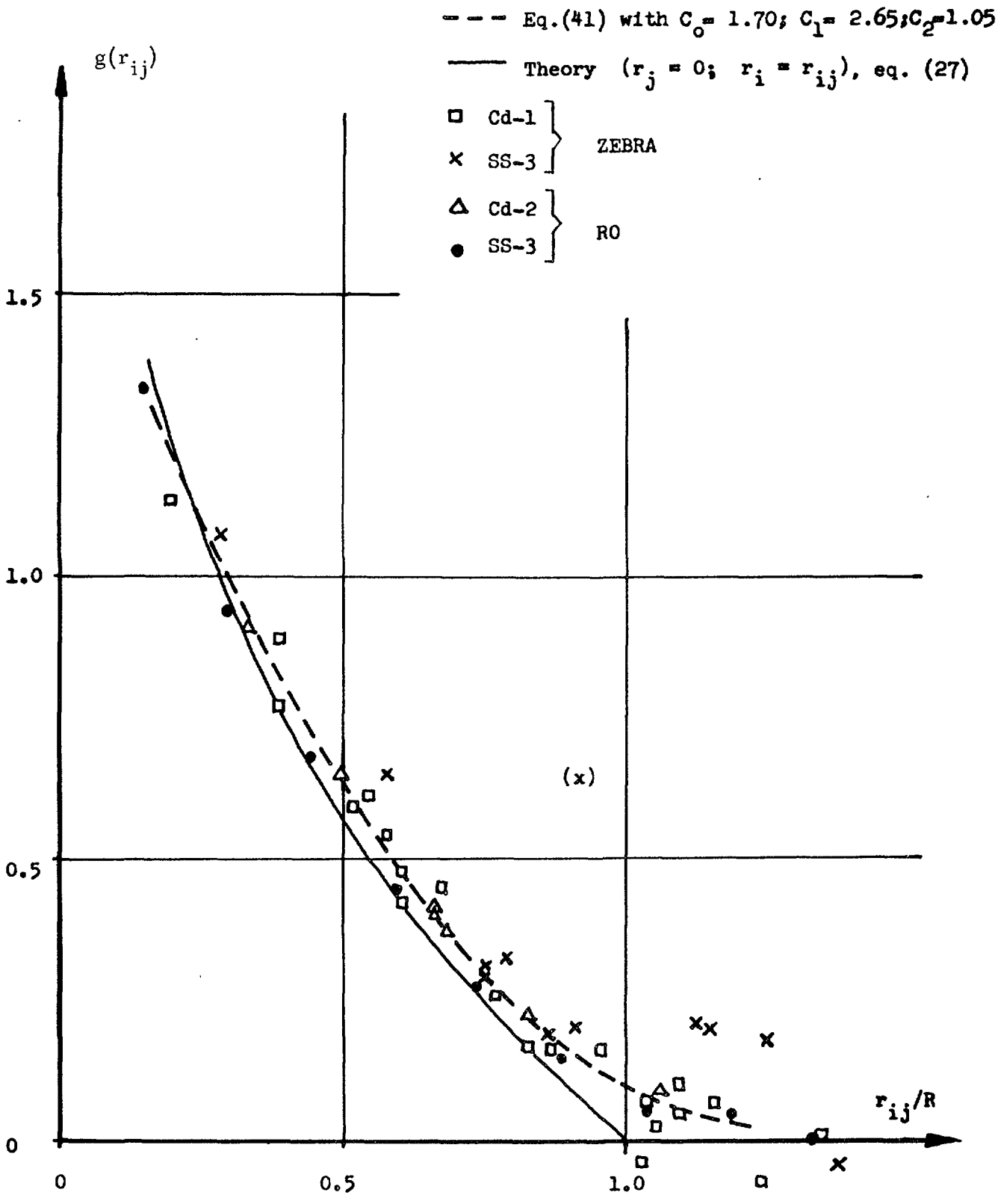

Fig. 7. The interaction function $g(r_{ij})$ versus the rod-to-rod spacing, r_{ij}/R

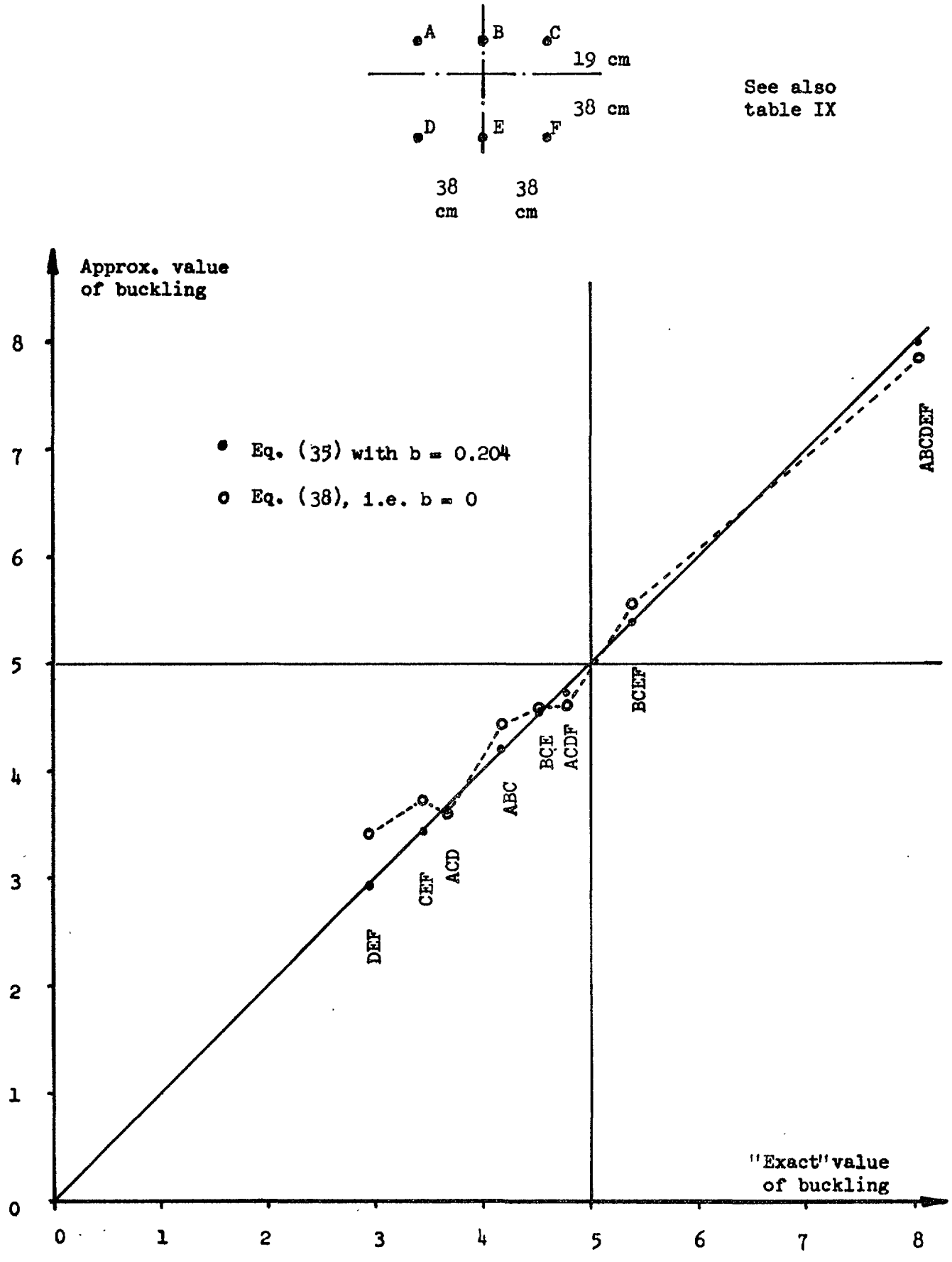

Fig. 8. Approximate values of buckling versus "exact" values with various combinations of control rods Cd-2 in R0

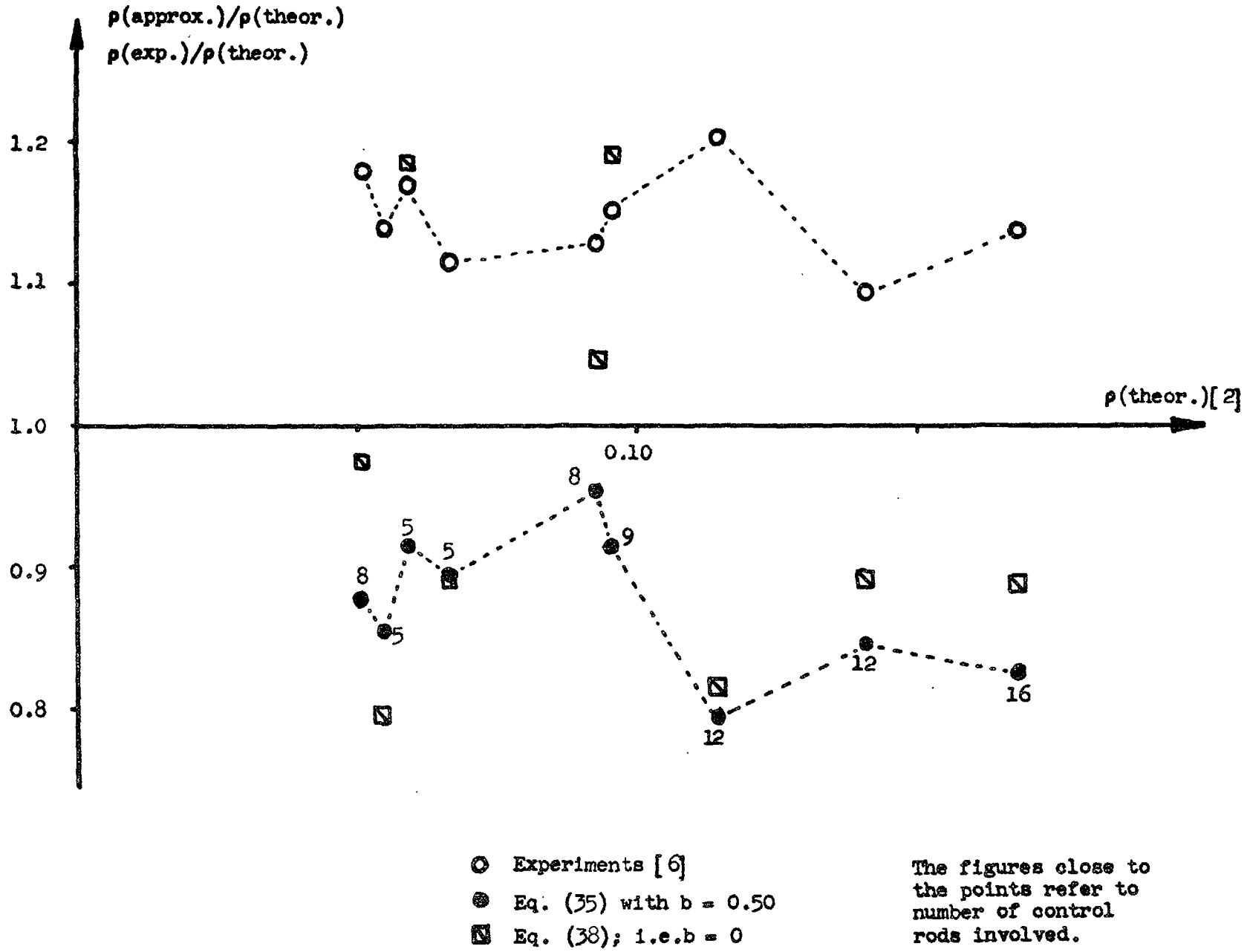

Fig. 9. Control rods in the Ågesta reactor. The reactivity ratios ρ(approx.)/ρ(theor.) and ρ(exp.)/ρ(theor.) vs ρ(theor.)

LIST OF PUBLISHED AE-REPORTS

1–170. (See the back cover earlier reports.)

171. Measurements on background and fall-out radioactivity in samples from the Baltic bay of Tvären, 1957–1963. By P. O. Agnedal. 1965. 48 p. Sw. cr. 8:–.

172. Recoil reactions in neutron-activation analysis. By D. Brune. 1965. 24 p. Sw. cr. 8:–.

173. A parametric study of a constant-Mach-number MHD generator with nuclear ionization. By J. Braun. 1965. 23 p. Sw. cr. 8:–.

174. Improvements in applied gamma-ray spectrometry with germanium semiconductor detector. By D. Brune, J. Dubois and S. Hellström. 1965. 17 p. Sw. cr. 8:–.

175. Analysis of linear MHD power generators. By E. A. Witalis. 1965. 37 p. Sw. cr. 8:–.

176. Effect of buoyancy on forced convection heat transfer in vertical channels – a literature survey. By A. Bhattacharyya. 1965. 27 p. Sw. cr. 8:–.

177. Burnout data for flow of boiling water in vertical round ducts, annuli and rod clusters. By K. M. Becker, G. Hernborg, M. Bode and O. Erikson. 1965. 109 p. Sw. cr. 8:–.

178. An analytical and experimental study of burnout conditions in vertical round ducts. By K. M. Becker. 1965. 161 p. Sw. cr. 8:–.

179. Hindered El transitions in Eu^{155} and Tb^{161}. By S. G. Malmskog. 1965. 19 p. Sw. cr. 8:–.

180. Photomultiplier tubes for low level Cerenkov detectors. By O. Strindehag. 1965. 25 p. Sw. cr. 8:–.

181. Studies of the fission integrals of U235 and Pu239 with cadmium and boron filters. By E. Hellstrand. 1965. 32 p. Sw. cr. 8:–.

182. The handling of liquid waste at the research station of Studsvik, Sweden. By S. Lindhe and P. Linder. 1965. 18 p. Sw. cr. 8:–.

183. Mechanical and instrumental experiences from the erection, commissioning and operation of a small pilot plant for development work on aqueous reprocessing of nuclear fuels. By K. Jönsson. 1965. 21 p. Sw cr. 8:–.

184. Energy dependent removal cross-sections in fast neutron shielding theory. By H. Grönroos. 1965. 75 p. Sw. cr. 8:–.

185. A new method for predicting the penetration and slowing-down of neutrons in reactor shields. By L. Hjärne and M. Leimdörfer. 1965. 21 p. Sw. cr. 8:–.

186. An electron microscope study of the thermal neutron induced loss in high temperature tensile ductility of Nb stabilized austenitic steels. By R. B. Roy. 1965. 15 p. Sw. cr. 8:–.

187. The non-destructive determination of burn-up means of the Pr-144 2.18 MeV gamma activity. By R. S. Forsyth and W. H. Blackadder. 1965. 22 p. Sw. cr. 8:–.

188. Trace elements in human myocardial infarction determined by neutron activation analysis. By P. O. Wester. 1965. 34 p. Sw. cr. 8:–.

189. An electromagnet for precession of the polarization of fast-neutrons. By O. Aspelund, J. Björkman and G. Trumpy. 1965. 28 p. Sw. cr. 8:–.

190. On the use of importance sampling in particle transport problems. By B. Eriksson. 1965. 27 p. Sw. cr. 8:–.

191. Trace elements in the conductive tissue of beef heart determined by neutron activation analysis. By P. O. Wester. 1965. 19 p. Sw. cr. 8:–.

192. Radiolysis of aqueous benzene solutions in the presence of inorganic oxides. By H. Christensen. 12 p. 1965. Sw. cr. 8:–.

193. Radiolysis of aqueous benzene solutions at higher temperatures. By H. Christensen. 1965. 14 p. Sw. cr. 8:–.

194. Theoretical work for the fast zero-power reactor FR-0. By H. Häggblom. 1965. 46 p. Sw. cr. 8:–.

195. Experimental studies on assemblies 1 and 2 of the fast reactor FR0. Part 1. By T. L. Andersson, E. Hellstrand, S-O. Londen and L. I. Tirén. 1965. 45 p. Sw. cr. 8:–.

196. Measured and predicted variations in fast neutron spectrum when penetrating laminated Fe-D_2O. By E. Aalto, R. Sandlin and R. Fräki. 1965. 20 p. Sw. cr. 8:–.

197. Measured and predicted variations in fast neutron spectrum in massive shields of water and concrete. By E. Aalto, R. Fräki and R. Sandlin. 1965. 27 p. Sw. cr. 8:–.

198. Measured and predicted neutron fluxes in, and leakage through, a configuration of perforated Fe plates in D_2O. By E. Aalto. 1965. 23 p. Sw. cr. 8:–.

199. Mixed convection heat transfer on the outside of a vertical cylinder. By A. Bhattacharyya. 1965. 42 p. Sw. cr. 8:–.

200. An experimental study of natural circulation in a loop with parallel flow test sections. By R. P. Mathisen and O. Eklind. 1965. 47 p. Sw. cr. 8:–.

201. Heat transfer analogies. By A. Bhattacharyya. 1965. 55 p. Sw. cr. 8:–.

202. A study of the "384" KeV complex gamma emission from plutonium-239. By R. S. Forsyth and N. Ronqvist. 1965. 14 p. Sw. cr. 8:–.

203. A scintillometer assembly for geological survey. By E. Dissing and O. Landström. 1965. 16 p. Sw. cr. 8:–.

204. Neutron-activation analysis of natural water applied to hydrogeology. By O. Landström and C. G. Wenner. 1965. 28 p. Sw. cr. 8:–.

205. Systematics of absolute gamma ray transition probabilities in deformed odd-A nuclei. By S. G Malmskog. 1965. 60 p. Sw. cr. 8:–.

206. Radiation induced removal of stacking faults in quenched aluminium. By U Bergenlid. 1965. 11 p. Sw. cr. 8:–.

207. Experimental studies on assemblies 1 and 2 of the fast reactor FR0. Part 2. By E. Hellstrand, T. Andersson, B. Brunfelter, J. Kockum, S-O. Londen and L. I. Tirén. 1965. 50 p. Sw. cr. 8:–.

208. Measurement of the neutron slowing-down time distribution at 1.46 eV and its space dependence in water. By E. Möller. 1965. 29 p. Sw. cr. 8:–.

209. Incompressible steady flow with tensor conductivity leaving a transverse magnetic field. By E. A. Witalis. 1965. 17 p. Sw. cr. 8:–.

210. Methods for the determination of currents and fields in steady two-dimensional MHD flow with tensor conductivity. By E. A. Witalis. 1965. 13 p. Sw. cr. 8:–.

211. Report on the personnel dosimetry at AB Atomenergi during 1964. By K. A. Edvardsson. 1966. 15 p. Sw. cr. 8:–.

212. Central reactivity measurements on assemblies 1 and 3 of the fast reactor FR0. By S-O. Londen. 1966. 58 p. Sw. cr. 8:–.

213. Low temperature irradiation applied to neutron activation analysis of mercury in human whole blood. By D. Brune. 1966. 7 p. Sw. cr. 8:–.

214. Characteristics of linear MHD generators with one or a few loads. By E. A. Witalis. 1966. 16 p. Sw. cr. 8:–.

215. An automated anion-exchange method for the selective sorption of five groups of trace elements in neutron-irradiated biological material. By K. Samsahl. 1966. 14 p. Sw. cr. 8:–.

216. Measurement of the time dependence of neutron slowing-down and thermalization in heavy water. By E. Möller. 1966. 34 p. Sw. cr. 8:–.

217. Electrodeposition of actinide and lanthanide elements. By N-E. Bärring. 1966. 21 p. Sw. cr. 8:–.

218. Measurement of the electrical conductivity of He^3 plasma induced by neutron irradiation. By J. Braun and K. Nygaard. 1966. 37 p. Sw. cr. 8:–.

219. Phytoplankton from Lake Magelungen, Central Sweden 1960–1963. By T. Willén. 1966. 44 p. Sw. cr. 8:–.

220. Measured and predicted neutron flux distributions in a material surrounding av cylindrical duct. By J. Nilsson and R. Sandlin. 1966. 37 p. Sw. cr. 8:–.

221. Swedish work on brittle-fracture problems in nuclear reactor pressure vessels. By M. Grounes. 1966. 34 p. Sw. cr. 8:–.

222. Total cross-sections of U, UO_2 and ThO_2 for thermal and subthermal neutrons. By S. F. Beshai. 1966. 14 p. Sw. cr. 8:–.

223. Neutron scattering in hydrogenous moderators, studied by the time dependent reaction rate method. By L. G. Larsson, E, Möller and S. N. Purohit. 1966. 26 p. Sw. cr. 8:–.

224. Calcium and strontium in Swedish waters and fish, and accumulation of strontium-90. By P-O. Agnedal. 1966. 34 p. Sw. cr. 8:–.

225. The radioactive waste management at Studsvik. By R. Hedlund and A. Lindskog. 1966. 14 p. Sw. cr. 8:–.

226. Theoretical time dependent thermal neutron spectra and reaction rates in H_2O and D_2O. S. N. Purohit. 1966. 62 p. Sw. cr. 8:–.

227. Integral transport theory in one-dimensional geometries. By I. Carlvik. 1966. 65 p. Sw. cr. 8:–.

228. Integral parameters of the generalized frequency spectra of moderators. By S. N. Purohit. 1966. 27 p. Sw. cr. 8:–.

229. Reaction rate distributions and ratios in FR0 assemblies 1, 2 and 3. By T. L. Andersson. 1966. 50 p. Sw. cr. 8:–.

230. Different activation techniques for the study of epithermal spectra, applied to heavy water lattices of varying fuel-to-moderator ratio. By E. K. Sokolowski. 1966. 34 p. Sw. cr. 8:–.

231. Calibration of the failed-fuel-element detection systems in the Ågesta reactor. By O. Strindehag. 1966. 52 p. Sw. cr. 8:–.

232. Progress report 1965. Nuclear chemistry. Ed. by G. Carleson. 1966. 26 p. Sw. cr. 8:–.

233. A Summary Report on Assembly 3 of FR0. By T. L. Andersson, B. Brunfelter, P. F. Cecchi, E. Hellstrand, J. Kockum, S-O. Londen and L. I. Tirén. 1966. 34 p. Sw. cr. 8:–.

234. Recipient capacity of Tvären, a Baltic Bay. By P.-O. Agnedal and S. O. W. Bergström. 21 p. Sw. cr. 8:–.

235. Optimal linear filters for pulse height measurements in the presence of notise. By K. Nygaard. 16 p. Sw. cr. 8:–.

236. DETEC, a subprogram for simulation of the fast-neutron detection process in a hydro-carbonous plastic scintillator. By B. Gustafsson and O. Aspelund. 1966. 26 p. Sw. cr. 8:–.

237. Microanalys of fluorine contamination and its depth distribution in zircaloy by the use of a charged particle nuclear reaction. By E. Möller and N. Starfelt. 1966. 15 p. Sw. cr. 8:–.

238. Void measurements in the regions of sub-cooled and low-quality boiling. P. 1. By S. Z. Rouhani. 1966. 47 p. Sw. cr. 8:–.

239. Void measurements in the regions of sub-cooled and low-quality boiling. P. 2. By S. Z. Rouhani. 1966. 60 p. Sw. cr. 8:–.

240. Possible odd parity in ^{128}Xe. By L Broman and S. G. Malmskog. 1966. 10 p. Sw. cr. 8:–.

241. Burn-up determination by high resolution gamma spectrometry: spectra from slightly-irradiated uranium and plutonium between 400–830 keV. By R. S. Forsyth and N Ronqvist. 1966 22 p. Sw. cr. 8:–.

242. Half life measurements in ^{155}Gd. By S. G. Malmskog. 1966. 10 p. Sw. cr. 8:–.

243. On shear stress distributions for flow in smooth or partially rough annuli. By B. Kjellström and S. Hedberg. 1966. 66 p. Sw. cr. 8:–.

244. Physics experiments at the Ågesta power station. By G. Apelqvist, P.-Å. Bliselius, P. E. Blomberg, E. Jonsson and F. Åkerhielm. 1966. 30 p. Sw. cr. 8:–.

245. Intercrystalline stress corrosion cracking of inconel 600 inspection tubes in the Ågesta reactor. By B. Grönwall, L. Ljungberg, W. Hübner and W. Stuart. 1966. 26 p. Sw. cr. 8:–.

246. Operating experience at the Ågesta nuclear power station. By S. Sandström. 1966. 113 p. Sw. cr. 8:–.

247. Neutron-activation analysis of biological material with high radiation levels. By K. Samsahl. 1966. 15 p. Sw. cr. 8:–.

248. One-group perturbation theory applied to measurements with void. By R. Persson. 1966. 19 p. Sw. cr. 8:–.

249. Optimal linear filters. 2. Pulse time measurements in the presence of noise. By K. Nygaard. 1966. 9 p. Sw. cr. 8:–.

250. The interaction between control rods as estimated by second-order one-group perturbation theory. By R. Persson. 1966. 42 p. Sw. cr. 8:–.

Förteckning över publicerade AES-rapporter

1. Analys medelst gamma-spektrometri. Av D. Brune. 1961. 10 s. Kr 6:–.
2. Bestrålningsförändringar och neutronatmosfär i reaktortrycktankar – några synpunkter. Av M. Grounes. 1962. 33 s. Kr 6:–.
3. Studium av sträckgränsen i mjukt stål. Av G. Östberg och R. Attermo. 1963. 17 s. Kr 6:–.
4. Teknisk upphandling inom reaktorområdet. Av Erik Jonson. 1963. 64 s. Kr 8:–.
5. Ågesta Kraftvärmeverk. Sammanställning av tekniska data, beskrivningar m. m. för reaktordelen. Av B. Lilliehöök. 1964. 336 s. Kr 15:–.
6. Atomdagen 1965. Sammanställning av föredrag och diskussioner. Av S. Sandström. 1966. 321 s. Kr 15:–.

Additional copies available at the library of AB Atomenergi, Studsvik, Nyköping, Sweden. Micronegatives of the reports are obtainable throught the International Documentation Center, Tumba, Sweden.

EOS-tryckerierna, Stockholm 1966